Electrosprayed gelatin submicroparticles as edible carriers for the encapsulation of polyphenols of interest in functional foods

*Laura G. Gómez-Mascaraque, José María Lagarón, Amparo López-Rubio**

Novel Materials and Nanotechnology Group, IATA-CSIC, Avda. Agustin Escardino 7, 46980 Paterna (Valencia), Spain

*Corresponding author: Tel.: +34 963900022; fax: +34 963636301
E-mail address: amparo.lopez@iata.csic.es (A. López-Rubio)

Other e-mail addresses: lggm@iata.csic.es (L. G. Gómez-Mascaraque), lagaron@iata.csic.es (J. M. Lagarón)

ABSTRACT

In this work, the potential of the electrospraying technique to obtain food-grade gelatin capsules in the submicron range for sensitive bioactive protection was explored, studying the influence of the protein concentration on the size and morphology of the obtained particles. Gelatin was selected as encapsulating material because, being commonly used as a food ingredient, it possesses unique gelation properties and is commercially available at a low cost. The electrosprayed matrices were used to encapsulate a model antioxidant molecule, (–)-epigallocatechin gallate (EGCG). Very high encapsulation efficiencies, close to 100%, were achieved, and the antioxidant activity of the bioactive was fully retained upon encapsulation. The EGCG release profiles showed a delayed release of the encapsulated antioxidant in aqueous solutions. Furthermore, while free EGCG in PBS lost a 30% of their antioxidant activity being completely degraded in 100 hrs, encapsulated EGCG retained its whole antioxidant activity within this time period.

KEYWORDS

Electrospray, encapsulation, gelatin, antioxidant, epigallocatechin gallate, functional food

Chemical compounds studied in this article:

(-)-Epigallocatechin gallate (PubChem CID: 65064)

1. Introduction

One of the main challenges in the development of functional foods is the preservation of the activity and bioavailability of the bioactive ingredients during food processing, storage and passage through the gastrointestinal tract. The development of edible nano- or microencapsulation matrices has been envisaged as a plausible option to protect these biologically active compounds against adverse conditions (Dube, Ng, Nicolazzo, & Larson, 2010a). There are a number of encapsulation techniques which can be used to produce nano- or microparticulate systems, being emulsification-evaporation, spray-drying and coacervation the most extensively used (López-Rubio, Sanchez, Wilkanowicz, Sanz, & Lagaron, 2012). However, some of these production methods involve exposure of the bioactives to high temperatures and/or the use of organic solvents, factors which can affect the stability of sensitive nutrients and preclude their use for food applications due to toxicity concerns associated with the residual traces of solvents (López-Rubio & Lagaron, 2011).

Electrospraying (e-spraying) has recently emerged as an alternative for the generation of polymeric particles incorporating bioactive agents (Bock, Dargaville, & Woodruff, 2012) with application in therapeutics, cosmetics and the food industry (Jaworek & Sobczyk, 2008). E-spraying, together with electrospinning (e-spinning), are versatile electrohydrodynamic fabrication methods which can generate encapsulation structures in a one-step process (Chakraborty, Liao, Adler, & Leong, 2009) without the need of employing high temperatures or toxic solvents (López-Rubio & Lagaron, 2012). A polymer solution flowing out from a nozzle is subjected to an external electrical field in such a way that when the electrical forces overcome the forces of surface tension, a charged jet is ejected towards a grounded collector. During the flight, the jet is elongated and the solvent evaporates, producing dry continuous fibres in the case of e-spinning (Bhardwaj & Kundu, 2010). In e-spraying, the jet breaks down into fine droplets which acquire spherical shapes due to the surface tension (Chakraborty et al., 2009), subsequently producing solid nano- or microparticles upon solvent evaporation. Apart from the feasibility of working at mild ambient conditions and using food-grade solvents, e-spraying has many other advantages as compared to other encapsulation techniques, including high encapsulation efficiencies, uniform bioactive distribution in the matrix, ease of operation and industrial scalability (Bock et al., 2012; Chakraborty et al., 2009). Moreover, particles aggregation could be prevented due to their own mutual

electrical repulsion, and smaller droplet sizes than in conventional mechanical atomisers can be obtained (Jaworek et al., 2008).

Among the different food-grade biopolymers which may be used as encapsulating materials, protein hydrogels are of particular interest as they are readily used as food ingredients, for instance to modify food texture or sensorial properties (Nieuwland et al., 2013). Specifically, gelatin has been widely employed for enhancing elasticity, stability and consistency of food products (Okutan, Terzi, & Altay, 2014). Moreover, it has been traditionally used by the pharmaceutical industry for the manufacture of hard and soft capsules to protect drugs from external agents such as atmospheric oxygen (Roussenova et al., 2012). Gelatin is obtained from partial hydrolysis of collagen which contains repeating sequences of glycine-aa_1-aa_2, where amino acids aa_1 and aa_2 are mainly proline and hydroxyproline (see Figure 1) (Lai, 2013). This biopolymer has drawn much research attention also in the field of controlled release of drugs due to its biodegradability and electrical properties, and because of its commercial availability and low cost (Lai, 2013; Okutan et al., 2014). One of the most interesting properties of gelatin is its ability to form thermoreversible hydrogels in water due to the formation of collagen-like triple helices, interconnected with amorphous regions of randomly coiled segments, and subsequent chains entanglement and network formation below the so-called helix–coil transition temperature (Peña, de la Caba, Eceiza, Ruseckaite, & Mondragon, 2010; Strauss & Gibson, 2004). This characteristic of the polypeptide makes it ideal to be processed in aqueous media, while avoiding complete disruption of the obtained capsules when submerged in aqueous foods below its gel-sol transition temperature.

However, gelatin cannot be e-sprayed at room temperature when dissolved in water (Huang, Zhang, Ramakrishna, & Lim, 2004) as gelation would occur (Erencia, Cano, Tornero, Macanás, & Carrillo, 2014). Different solvents, such as fluoroalcohols (Huang et al., 2004), have been suggested as alternatives to process gelatin by e-spinning/spraying with positive results, but their high toxicity limits their use for food applications. The use of diluted carboxylic acids (Ki et al., 2005; Songchotikunpan, Tattiyakul, & Supaphol, 2008) or ethyl acetate (Song, Kim, & Kim, 2008) has also been proposed as non-toxic solvents in various works. Particularly, e-spinning of gelatin solutions in acetic acid has been previously reported for type B gelatin from bovine skin (Erencia et al., 2014; Okutan et al., 2014).

Green tea polyphenols are powerful antioxidants which have attracted great interest in the field of functional foods due to their numerous attributed health benefits. (–)-Epigallocatechin gallate (EGCG), the most abundant and biologically active compound in green tea (Barras et al., 2009), was selected in this work as a model antioxidant molecule due to its numerous attributed health benefits. It has shown protective effects against infections (Steinmann, Buer, Pietschmann, & Steinmann, 2013), cardiovascular and neurodegenerative diseases (Fu et al., 2011), inflammation and arthritis (Singh, Akhtar, & Haqqi, 2010) and cancer (Larsen & Dashwood, 2009, 2010; Singh, Shankar, & Srivastava, 2011), among other therapeutic benefits. However, its poor stability in aqueous solutions (Dube, Nicolazzo, & Larson, 2010b; Li, Lim, & Kakuda, 2009) limits its direct addition to food products. Several carrier systems have been developed to protect EGCG from degradation (Barras et al., 2009; Dube et al., 2010b; Folch-Cano, Jullian, Speisky, & Olea-Azar, 2010; Li et al., 2009; Rocha et al., 2011; Ru, Yu, & Huang, 2010).

In this work, for the first time, e-sprayed gelatin micro- and submicroparticles are proposed as food-grade encapsulating matrices for EGCG. A type A gelatin from porcine skin was selected in order to confirm whether previous results on the processability of bovine type B gelatin in diluted acetic acid could be applicable to a gelatin from a different origin. Thus, gelatin micro- and submicroparticles were produced in food-grade conditions by electrohydrodynamic treatment, and their ability for the encapsulation and stabilization of bioactives was studied using EGCG as a model water-soluble antioxidant.

INSERT FIGURE 1 ABOUT HERE

2. Materials and Methods

2.1. Materials

Type A gelatin from porcine skin (Gel), with reported gel strength of 175 g Bloom was obtained from Sigma-Aldrich. (–)-Epigallocatechin gallate (EGCG), 2,2'-azino-bis(3-ethylbenzothiazoline-6-sulfonic acid) diammonium salt (ABTS), buffer solutions of pH 7.4 (phosphate buffered saline system, PBS) and pH 6.1 (2-(N-morpholino)ethanesulfonic acid hemisodium salt, MES), potassium persulfate ($K_2O_8S_2$) and potassium bromide FTIR grade (KBr) were also obtained from Sigma-Aldrich. 96% (v/v) acetic acid (Scharlab) and 96% (v/v) ethanol (Panreac) were used as received.

137

138 **2.2. Preparation of gelatin solutions**

139 Gelatin aqueous solutions of different concentrations, i.e. 5, 8, 10 and 20% (w/v), were
140 prepared by dissolving the biopolymer in acetic acid 20% (v/v) at 40ºC under magnetic
141 agitation, and cooled down to room temperature before processing. Gelation of the
142 solutions was not observed for any of the samples.
143 When EGCG was incorporated for its encapsulation, it was added to the gelatin
144 solutions at room temperature under magnetic stirring, at a concentration of 10 wt.-% of
145 the total solids content.

146

147 **2.3. Characterization of the solutions**

148 The surface tension of the solutions was measured using the Wilhemy plate
149 method in an EasyDyne K20 tensiometer (Krüss GmbH, Hamburg, Germany) at room
150 temperature.
151 The electrical conductivity of the solutions was measured using a conductivity meter
152 XS Con6 (Labbox, Barcelona, Spain) at room temperature.
153 The rheological behaviour of the solutions was studied using a rheometer model AR-G2
154 (TA Instruments, USA), with a parallel plate geometry. The stainless steel plate
155 diameter was 60 mm and the gap was fixed to 0.5 mm. The tests were performed at a
156 controlled temperature of 25ºC ± 0.1ºC. Continuous shear rate ramps were performed
157 from 0.1 to 200 s^{-1} during 15 min after equilibrating the samples for 5 min, and the
158 shear stress of the samples was registered. All measurements were made at least in
159 triplicate.

160

161 **2.4. Electrohydrodynamic processing of the solutions**

162 The solutions were processed using a Fluidnatek® LE-10 electrospinning/
163 electrospraying apparatus, equipped with a variable high voltage 0–30 kV power
164 supply, purchased from BioInicia S.L. (Valencia, Spain). Solutions were introduced in
165 a 5 mL plastic syringe and were pumped at a steady flow-rate through a stainless-
166 steel needle (0.9 mm of inner diameter). The needle was connected through a PTFE
167 wire to the syringe, which was placed on a digitally controlled syringe pump. Processed
168 samples were collected on a stainless-steel plate connected to the cathode of the power
169 supply and placed horizontally with respect to the syringe. The processing parameters
170 were empirically optimized for each gelatin concentration in order to attain stable

electrospraying avoiding dripping of the solution. Briefly, the flow rate varied from 0.15 to 0.5 mL/h and the voltage was maintained within the range 15-28 kV. The distance between the tip of the syringe and the collector was 10 cm in all cases.

2.5. Morphological characterization of the particles

Scanning electron microscopy (SEM) was conducted on a Hitachi microscope (Hitachi S-4100) at an accelerating voltage of 10 kV and a working distance of 9-16 mm. Samples were sputter-coated with a gold-palladium mixture under vacuum prior to examination. Particle diameters were measured from the SEM micrographs in their original magnification using the ImageJ software. Size distributions were obtained from a minimum of 200 measurements.

2.6. Fourier transform infrared (FT-IR) analysis of the particles

Empty and bioactive-containing capsules of ca. 1 mg were grounded and dispersed in 130 mg of spectroscopic grade potassium bromide (KBr). A pellet was then formed by compressing the sample at ca. 150 MPa. FT-IR spectra were collected in transmission mode using a Bruker (Rheinstetten, Germany) FT-IR Tensor 37 equipment. The spectra were obtained by averaging 10 scans at 1 cm^{-1} resolution.

2.7. Encapsulation efficiency

The encapsulation efficiency (EE) of the EGCG-loaded capsules was determined based on FT-IR absorbance measurements. A calibration curve (R^2 = 0.995) was obtained using gelatin/EGCG mixtures of known relative concentrations (0, 5, 10 and 15 % w/w of EGCG). The relative maximum absorbances at 1409 cm^{-1} (corresponding to gelatin) and 1039 cm^{-1} (attributed to EGCG) were plotted against the EGCG concentration in the mixtures (cf. Figure S1 in the supplementary material). The EGCG content in the capsules was interpolated from the obtained linear calibration equation. The EE of the EGCG-loaded capsules was then calculated using Eq. (1):

$$EE\ (\%) = \frac{Actual\ EGCG\ content\ in\ the\ capsules}{Theoretical\ EGCG\ content\ in\ the\ capsules} \times 100 \qquad \text{Eq. (1)}$$

2.8. Thermal Properties of the particles

Thermogravimetric analysis (TGA) was performed with a TA Instruments model Q500 TGA. The samples (ca. 8 mg) were heated from room temperature to 600ºC with a heating rate of 10ºC/min under dynamic air atmosphere. Derivative thermogravimetric (DTG) curves express the weight loss rate as a function of temperature.

2.9. EGCG release from the gelatin particles

10 mg of gelatin/EGCG capsules were suspended in 20 mL of release medium and kept at 20ºC under agitation in a Selecta thermostatic bath model Unitronic Reciprocal C (Barcelona, Spain). Three different release media were used: ethanol (96% v/v), MES aqueous buffer (pH=6.1) and PBS aqueous buffer (pH=7.4). At different time intervals, the suspensions were centrifuged at 3500 rpm and ambient temperature during 10 min using a centrifuge from Labortechnik model Hermle Z 400 K (Wasserburg, Germany), and 1 mL aliquot of the supernatant was removed for sample analysis. The aliquot volume was then replaced with fresh release medium and the particles re-suspended and left back in the thermostatic bath.

The extracted aliquots were analysed by UV-Vis spectroscopy (Shanghai Spectrum model SP-2000UV, Shanghai, China) by measuring the absorbance at 274 nm (maximum of absorbance of EGCG (Rocha et al., 2011)). Calibration curves for EGCG quantification in solution by UV-Vis absorbance were previously obtained for the three different release media ($R^2_{ethanol}$ = 0.998, R^2_{MES} = 0.999, R^2_{PBS} = 0.999). The EGCG release values were obtained from three independent experiments.

2.10. *In-vitro* antioxidant activity

$ABTS^{+\bullet}$ radical scavenging assay was performed in order to quantify the antioxidant activity of both free and encapsulated EGCG, following the decolourization assay protocol described by Re et al. (1999). Briefly, a stock solution of $ABTS^{+\bullet}$ was prepared by reacting ABTS with potassium persulfate (7 and 2.45 mM in distilled water, respectively) and allowing the mixture to stand in the dark at room temperature for 24 hrs. The $ABTS^{+\bullet}$ stock solution was then diluted with acetic acid 20% v/v (same solvent in which the samples were dissolved) to an absorbance of 0.70±0.02 at 734 nm. Stock solutions of free and encapsulated EGCG (5 mM of EGCG in both cases) were prepared in acetic acid 20% v/v to facilitate the dissolution of the gelatin matrix and subsequent complete release of EGCG from the capsules. Then, these stock solutions were diluted 20-fold. 10 μL of diluted sample solution were added to 1 mL of diluted $ABTS^{\bullet+}$, and

the absorbance at 734 nm measured at room temperature 1 min after initial mixing. The radical scavenging activity (RSA), expressed as the percentage of reduction of the absorbance at 734 nm after sample addition, was calculated using Eq. (2):

$$RSA\ (\%) = \frac{A_0 - A_1}{A_0} \times 100 \qquad \text{Eq. (2)}$$

Where A_0 and A_1 are the absorbances at 734 nm of $ABTS^{+\bullet}$ before and 1 min after addition of the antioxidant samples, respectively.

Experiments were performed on a Shanghai Spectrum spectrophotometer model SP-2000UV (Shanghai, China), at least in triplicate. Solvent blanks were also run in each assay. Unloaded gelatin particles were also evaluated (same particle concentration as in loaded samples) to take into account the potential antioxidant activity of the encapsulation matrix.

2.11. EGCG degradation assays

Solutions/suspensions of 5 mM EGCG and EGCG-loaded gelatin capsules with theoretical EGCG concentrations of 5 mM in PBS were prepared. After selected time intervals, the solutions/suspensions were diluted 20-fold with acetic acid 20% v/v and the $ABTS^{+\bullet}$ radical scavenging assay was conducted as previously explained. The radical scavenging activity (RSA) at the different time intervals was calculated using eq. (2).

2.12. Statistical analysis

A statistical analysis of experimental data was performed through analysis of variance (one-way ANOVA) using OriginPro 8 (OriginLab Corp., Northampton, USA). Homogeneous sample groups were obtained by using Fisher LSD test (95% significance level, $p < 0.05$).

3. Results and discussion

3.1. Optimization of the e-spraying process for obtaining EGCG-loaded gelatin particles

Gelatin solutions were prepared in diluted acetic acid (20% v/v) to enable their processing using e-spraying, as premature gelation of the protein precludes capsule

formation using this technique. Moreover, this solvent was considered appropriate for the expected final application as it does not leave toxic residues on the dry materials (Klossner, Queen, Coughlin, & Krause, 2008). Under these food-grade conditions, gelation of the solutions was not observed for any of the samples during the electrohydrodynamic processing at room temperature.

Different material morphologies can be obtained through electrohydrodynamic processing of polymer solutions depending on the process parameters and the solution properties. For food applications, particles rather than fibres are preferred, since they are easier to handle and to subsequently disperse within the food products. Therefore, various concentrations of gelatin were tested in order to optimize the e-spraying process, with the objective to obtain neat individual particles as free of residual fibrils as possible. Electrohydrodynamic processing of bovine type B gelatin solutions in acetic acid had been previously attempted (Erencia et al., 2014; Okutan et al., 2014), and the reported results served as a starting point to select a set of protein concentrations to be tested for the optimization of the e-spraying process for type A gelatin from porcine origin. Four different gelatin concentrations (5, 8, 10 and 20% w/v, with sample codes Gel5, Gel8, Gel10 and Gel20, respectively) were finally selected, and the processing parameters (i.e. flow rate and voltage) were also adjusted to maximize the production rate while keeping a stabilized jet, thus, avoiding dripping of the solution. The optimal processing parameters found in this study for the different compositions are summarized in Table 1.

INSERT TABLE 1 ABOUT HERE

The size and morphology of materials obtained through electrohydrodynamic processing is strongly dependent on the properties of the polymer solutions (Pérez-Masiá, Lagaron, & López-Rubio, 2014). Thus, the selected gelatin solutions were characterized in terms of surface tension, electrical conductivity and rheological behaviour prior to their processing and the results are summarized in Figure 2.

INSERT FIGURE 2 ABOUT HERE

Figure 3 shows the morphology of the processed structures obtained from the different solutions together with the particle size distributions for the e-sprayed samples.

INSERT FIGURE 3 ABOUT HERE

Fibres were obtained for the sample with the greatest protein concentration (i.e. Gel20), while pseudo-spherical particles typical of the discontinuous e-spraying process, with more or less residual fibrils, were produced for lower gelatin concentrations. These results are consistent with the electrospinnability domains recently established by Erencia et al. (2014) for gelatin-water-acetic acid systems using a type B gelatin from bovine skin (Erencia et al., 2014). A certain protein concentration is needed to establish the necessary peptide chain entanglements and chain-chain interactions leading to fibre formation. The particle size distributions of the e-sprayed samples (cf. Figure 3) reflected a decrease in the particle diameter and greater heterogeneity of capsule sizes as the gelatin concentration decreased. In all cases, the majority of the particles had a size in the submicron range, having their maximum in the nanoscale.

Regarding the solution properties, in general, a slight increase in the conductivity of the solutions was observed with the polymer concentration, whereas no significant variation was observed for their surface tension. Therefore, differences in the morphology of the processed materials could be mainly attributed to changes in the rheological properties of the solutions. All tested solutions exhibited a Newtonian behaviour, with a linear relationship between the shear stress and the shear rate in the whole range of study (cf. Figure 2) and, thus, the viscosity was calculated from the slope of the shear stress vs. shear rate curves. The Newtonian behaviour of gelatin in aqueous solutions, even at high concentrations, had been previously reported at neutral pH (Wulansari, Mitchell, Blanshard, & Paterson, 1998). As expected, the viscosity exponentially increased with the gelatin concentration (Erencia et al., 2014), which resulted in sample Gel20 having a viscosity considerably higher than the rest of the samples and above the so-called critical entanglement concentration, defined as the crossover of concentration from the semidilute unentangled to the semidilute entangled regimes in polymeric solutions (Gupta, Elkins, Long, & Wilkes, 2005). The presence of sufficient chain entanglements for a 20% gelatin concentration explains the production of e-spun fibres instead of e-sprayed particles (Shenoy, Bates, Frisch, & Wnek, 2005) in sample Gel20, as jet fragmentation during processing was prevented by the strong intermolecular cohesion of this concentrated solution (Chakraborty et al., 2009).

The most spherical morphology, almost free of residual fibrils, was exhibited by Gel8. Higher concentrations led to fibrils formation while lower concentrations resulted in

some dripping of the solution. Hence, this gelatin concentration was selected as optimal for further experiments.

Once the conditions for the production of e-sprayed gelatin capsules were optimized, these vehicles were loaded with EGCG as a model water-soluble antioxidant. The gelatin solution (8% w/v) was prepared as in previous experiments, and EGCG was subsequently added at room temperature to achieve a final theoretical EGCG concentration of 10% w/w in the capsules. The morphology and particle size distribution of the resulting encapsulates was similar to those of their unloaded counterparts (cf. Figure 3). A very similar morphology with slightly rougher surface of the capsules was observed for the loaded structures, as solution properties were not considerably affected upon EGCG addition (cf. Figure 2).

3.2. Molecular organization and encapsulation efficiency

The e-sprayed gelatin capsules, both unloaded and loaded with EGCG, were characterized by FTIR spectroscopy along with the commercial untreated gelatin and EGCG.

The spectrum of commercial gelatin showed its four most characteristic bands centred at 3430 cm^{-1} (Amide A, NH stretching), 1642 cm^{-1} (Amide I, C=O and CN stretching), 1543 cm^{-1},(Amide II, N-H bending) and 1244 cm^{-1} (Amide III, C-N stretching) (Aewsiri, Benjakul, Visessanguan, Wierenga, & Gruppen, 2010; Gomes, Rodrigues, Martins, Henriques, & Silva, 2013; Li, Miao, Wu, Chen, & Zhang, 2014). Also, a band corresponding to the asymmetric stretching vibration of =C–H and $–NH_3^+$ (Amide B) was observed at 3085 cm^{-1} (Nagarajan, Benjakul, Prodpran, Songtipya, & Nuthong, 2013). The bands observed at 2960 and 2928 cm^{-1} correspond to CH_2 asymmetric and symmetric stretching vibrations, respectively, mainly from the glycine backbone and proline side-chains (Nagarajan et al., 2013; Nagiah, Madhavi, Anitha, Srinivasan, & Sivagnanam, 2013).

After the e-spraying treatment, sample Gel8 exhibited the same characteristic bands as the commercial gelatin, but a considerable narrowing and better definition of the bands was apparent, which has been previously observed for other biopolymers after capsule formation (Pérez-Masiá et al., 2014). Moreover, significant displacements were detected for the bands corresponding to the Amides A and I from 3430 and 1642 cm^{-1} to 3402 and 1653 cm^{-1}, respectively, which can be attributed to differences in hydrogen bonding and protein conformation (Nagarajan et al., 2013) caused by the e-spraying processing.

Specifically, shifts of the Amide A band to lower wavenumbers indicate hydrogen bond formation via the N-H groups of the peptides (Doyle, Bendit, & Blout, 1975), while the shift of the amide I band to 1653 cm^{-1} can be correlated with β-sheet peptide conformation as previously observed for other proteins (Ebrahimgol, Tavanai, Alihosseini, & Khayamian, 2014).

The spectrum of commercial EGCG showed an intense band at 3358 cm^{-1} due to the stretching of O-H groups, and other characteristic bands at 1618 cm^{-1}, attributed to the aromatic ring quadrant, at 1544, 1528 and 1518 cm^{-1}, corresponding to the aromatic semicircle stretch, at 1294 cm^{-1}, due to the deformation vibration of O-H groups of the aromatic alcohol, and at 1097 cm^{-1}, owed to the aromatic rings stretch (Robb, Geldart, Seelenbinder, & Brown, 2002). The presence of EGCG in the loaded capsules was evidenced by the existence of absorption bands corresponding to this polyphenol in their infrared spectrum, in particular the bands at 1042 cm^{-1} (which shifted to 1038 cm^{-1} in the capsules) and 1148 cm^{-1} (cf. arrows in the inset of Figure 4).

Proteins have been described to strongly interact with polyphenol molecules through hydrogen bonding and hydrophobic interactions (Li et al., 2009; Peña et al., 2010). In the e-sprayed loaded gelatin particles developed in this work, apart from the displacement of the 1042 cm^{-1} band of the EGCG, other changes were observed in the infrared spectrum from gelatin upon encapsulation of the bioactive compound. For instance, the maximum of the Amide A band shifted to even lower wavenumbers (3358 cm^{-1}), thus suggesting, as previously explained, that hydrogen bonding between the gelatin matrix and the bioactive took place. The Amide III band also shifted from 1245 cm^{-1} in Gel8 to 1241 cm^{-1} in the EGCG-loaded capsules. These differences suggest the presence of intermolecular interactions between the antioxidant and the biopolymer within the developed capsules, which might contribute to the stabilization of the former.

INSERT FIGURE 4 ABOUT HERE

Infrared spectroscopy was also used to estimate the encapsulation efficiency of the samples. Based on the measurements of absorbance intensities from the isolated spectral bands from the protein matrix and the bioactive at 1409 cm^{-1} and 1039 cm^{-1}, respectively, a calibration curve ($R^2 = 0.995$) was constructed using physical mixtures of gelatin and EGCG of known relative concentrations (cf. Figure S1 in the Supplementary data). The EE of the EGCG-loaded capsules was 96% ± 3%, i.e., almost all the

antioxidant added to the solution was effectively incorporated within the capsules. This value was considerably higher than those reported for other encapsulation systems for the protection of cathequins (Dube et al., 2010b; Fang, Hwang, Huang, & Fang, 2006; Hu, Ting, Zeng, & Huang, 2013; Shpigelman, Cohen, & Livney, 2012) and can be explained taking into account the great solubility of EGCG in the polymeric solution and the absence of partitioning effects (Dube et al., 2010b) when using e-spraying as the encapsulation technique.

3.3. TGA. Thermal stability of the particles.

Thermogravimetric analysis of raw materials and electrosprayed particles (Gel 8% w/v, both empty and EGCG-loaded), were performed in order to study possible thermostability changes of the ingredients upon electrohydrodynamic treatment. Table 2 and Figure 5 summarize the main results.

Three different stages were observed in the weight loss curve of gelatin. The first stage, observed at temperatures up to 200ºC, is related to the loss of adsorbed and bound water present in the gelatin samples due to its hygroscopic character. The second stage, corresponding to the major weight loss, occurred between 200 and 400°C and has been associated with the protein chain rupture and peptide bonds breakage (Inamura et al., 2013). The last stage, observed between 400ºC and 600ºC, has been attributed to the thermal decomposition of the gelatin networks (Correia et al., 2013). Other authors relate these second and third stages to the elimination of aminoacid fragments in oxidant atmosphere, mainly proline, and the degradation of glycine, respectively (Aquino et al., 2012).

INSERT TABLE 2 ABOUT HERE

The thermogravimetric curves of the e-sprayed gelatin particles showed similar degradation profiles to that of the original gelatin powder. However, slight changes in the degradation profile of the main stage were observed. The temperature of maximum degradation rate of this stage (T_{max1}) increased upon e-spraying of the protein, both in the presence and in the absence of antioxidant, although degradation was extended over a wider range of temperatures. Specifically, a slight decrease in the onset temperature (T_{onset}) was observed, which cannot be ascribed to EGCG degradation as it was also seen for the unloaded structures.

INSERT FIGURE 5 ABOUT HERE

Regarding the water loss during the first stage, noticeable differences were observed between unprocessed and e-sprayed gelatin samples. Different types of water bound to proteins have been reported (Correia et al., 2013), including absorbed and structural water. Absorbed water is removed from the samples up to 100ºC, while structural water needs more energy and is eliminated at higher temperatures. Figure 5 shows that, while the first weight loss stage of raw gelatin was extended up to 200ºC due to the presence of structural water, the water loss of e-sprayed gelatin samples, both loaded and unloaded, was only seen up to 100ºC, suggesting that only absorbed water was present in these samples. In fact, the weight loss in this first step was greater for raw gelatin (9.5%) than for both e-sprayed materials (7.2% for Gel8 and 6.0% for Gel8-EGCG). These findings support that the fast drying of the samples during electrohydrodynamic processing of gelatin solutions is capable of removing structural water from the protein, and promoting hydrogen bonding between polypeptide chains and also between the protein and the polyphenol molecules as observed by infrared spectroscopy.

No peaks attributed to the degradation of EGCG were detected in the TGA curve of the EGCG-loaded capsules. This could be explained by the good compatibility and intermolecular interactions between the polymer and the bioactive, as previously inferred from the infrared results, which contributed to the stabilization of the latter until the protecting matrix was degraded.

3.4. EGCG release from the electrosprayed gelatin particles

The release of EGCG from the e-sprayed gelatin capsules was studied in three different media. PBS aqueous buffer (pH=7.4) was selected as a simulated biological fluid, as it is one of the most commonly used blood plasma simulant (Singh, Sharma, & Majumdar, 2013). On the other hand, ethanol is a good simulant for fatty foods and it is easy to work with analytically (Baner, Bieber, Figge, Franz, & Piringer, 1992; Cooper, Goodson, & O'Brien, 1998), so it was selected as a fatty food simulant, while MES aqueous buffer (pH=6.1) was selected as a simulant for slightly acidic aqueous foods such as juices (Tola & Ramaswamy, 2014).

The resulting release profiles are depicted in Figure 6. An initial burst release was observed in all tested media, followed by a slower sustained release which was more

clearly observed in the ethanolic suspension. The release was faster in aqueous media as a consequence of the swelling of the gelatin matrix, but still, due to the encapsulation of the antioxidant molecule its dissolution in these media was delayed. This will consequently impact on the degradation kinetics in solution.

INSERT FIGURE 6 ABOUT HERE

A number of semi-empirical mathematical models have been proposed in the literature to describe the release kinetics of bioactive molecules from a carrier or delivery system (Siepmann & Peppas, 2012), and some of the most commonly used ones have been applied to the experimental data in Figure 6, including the Higuchi equation (Higuchi, 1961), the power law model or Ritger-Peppas semiempirical equation (Ritger & Peppas, 1987), and the Peppas-Sahlin model (Peppas & Sahlin, 1989). The last two take into account the combination of Fickian (diffusion) and non-Fickian (polymer relaxation) release mechanisms. These models usually fit experimental data only in the early time points of the release profile (Ritger et al., 1987), and thus only the data corresponding to the so called 'burst release phase' (Gallagher & Corrigan, 2000) was fitted to the models.

The Peppas-Sahlin model was the one which better fitted our experimental data. Its general equation is shown in Eq. (3), where M_t is the mass of EGCG released at time t, M_0 is the total mass of EGCG loaded in the particles, m is the Fickian diffusional exponent, and k_i are kinetic constants (Siepmann et al., 2012). For an aspect ratio of 1 (i.e. spherical geometry of the carrier), m = 0.425 (Peppas et al., 1989). Table 3 shows the EGCG release kinetic parameters for the Peppas-Sahlin equation in the different food simulants.

$$\frac{M_t}{M_0} = k_1 \cdot t^m + k_2 \cdot t^{2m} \qquad \text{Eq. (3)}$$

INSERT TABLE 3 ABOUT HERE

The Peppas-Sahlin model allows estimation of the relative contribution of the relaxational phenomenon and the diffusional mechanism on the release kinetics. The first term of the equation ($k_1 \cdot t^m$) accounts for the contribution of the diffusion

phenomenon to the EGCG release kinetics, while the second term ($k_2 \cdot t^{2m}$) accounts for the case-II transport (Peppas et al., 1989; Spizzirri et al., 2013). For the e-sprayed gelatin particles, k_1 was greater than k_2 in the three food simulants, suggesting that the diffusional mechanism was predominant. Similar behavior has been reported for other spherical carriers based on gelatin microgels (Spizzirri et al., 2013). The ratio k_1/k_2 was higher for the release of EGCG in ethanol than in the aqueous media, indicating that the swelling or relaxation of the gelatin matrix had a greater contribution to the release kinetics in the aqueous food simulants, as expected. Moreover, the release was also much faster in these media, as confirmed by the higher values of the kinetic constants in MES and PBS.

3.5. *In-vitro* antioxidant activity and degradation assays

$ABTS^{+\bullet}$ decolourization assay was performed in order to compare the antioxidant activity of encapsulated and free EGCG. For this purpose, diluted acetic acid was used to disrupt the gelatin capsules and dissolve EGCG. The concentration of loaded capsules was calculated to have the same EGCG concentration as in the free EGCG sample (i.e. 0.25 mM), assuming 100% encapsulation efficiency. Unloaded e-sprayed gelatin particles were also evaluated in order to disregard possible contributions of the encapsulating matrix to the total antioxidant activity of the encapsulates, using the same particles concentration as for the loaded capsules. Solvent blanks were run too. The radical scavenging activity (RSA) of each antioxidant solution was calculated using eq. (2).

No statistically significant differences ($p < 0.05$) were observed between the inhibition of the absorbance caused by the e-sprayed gelatin matrix (RSA = 3.2 ± 0.2 %) and the solvent blank (RSA= 3.4 ± 0.2 %), so the whole antioxidant activity of the loaded capsules could be attributed to its EGCG content. The antioxidant activity of encapsulated EGCG (RSA = 26.8 ± 0.7 %) was not significantly different from that of free EGCG (RSA = 27.2 ± 1.5 %) either, thus confirming that the encapsulation efficiency was indeed very close to 100%, because the theoretical loading matched the experimental antioxidant activity of free EGCG. These results corroborated the previous estimations obtained from infrared spectroscopy measurements and verified that the e-spraying process did not damage the bioactive, as its antioxidant activity was kept intact.

The $ABTS^{+\bullet}$ decolourization assay was also used to study the degradation of free and encapsulated EGCG in aqueous solution/suspension, by measuring the decrease in their RSA value with time as an indicative of the loss of their antioxidant activity due to degradation. PBS was the selected degradation media as EGCG is highly unstable in aqueous solution, especially in neutral or alkaline solutions (Barras et al., 2009; Li et al., 2009), suffering degradation through oxidative processes (Dube et al., 2010b). Hence, solutions 5 mM of EGCG and suspensions of EGCG-loaded capsules with the same theoretical EGCG concentration were prepared. Fast degradation of EGCG upon dissolution in PBS media could be clearly observed by its gradual transition from a light pink to an intense yellowish colour. At selected time intervals, the solutions/suspensions were diluted 20-fold with acetic acid 20% v/v with the double objective of disrupting the gelatin capsules and stopping the degradation process by acidification of the medium. The inhibition of the absorbance of $ABTS^{+\bullet}$ caused by the resulting solutions was measured and their RSA values calculated. The results are shown in Figure 7.

INSERT FIGURE 7 ABOUT HERE

The free EGCG samples lost a 30% of their initial RSA in 100 hrs. No further antioxidant activity loss was observed after longer time periods, suggesting that EGCG was fully degraded in PBS after 4 days, even though its degradation products also exhibited some antioxidant activity. In contrast, no significant loss of antioxidant activity was observed for the encapsulated molecule within an observation time of 10 days ($p < 0.05$). This finding proved that the encapsulation system proposed in this work was capable of protecting EGCG from degradation in slightly alkaline solutions.

1. Conclusions

Gelatin-based encapsulation matrices were produced from food-grade ingredients without the need of employing high temperatures or toxic solvents by electrohydrodynamic treatment of gelatin solutions in diluted acetic acid. The electrospraying process was initially optimized in order to obtain neat particles, almost free of fibrils, to facilitate handling and dispersion into food products. Pseudo-spherical particles with mean sizes in the submicron range were obtained. The potential of these particles to be used as edible carriers for the encapsulation and protection of a model, water-soluble antioxidant, EGCG, was tested by producing electrosprayed gelatin

574 particles with a theoretical antioxidant loading of 10% w/w. Infrared spectroscopy and
575 $ABTS^{\cdot+}$ assays revealed that the encapsulation efficiency of the system was very close
576 to 100%, much higher than that reported for other encapsulation systems for the
577 protection of catechins. Moreover, the radical scavenging assays proved that
578 encapsulation by the e-spraying technique did not damage the bioactive compound, as it
579 retained its antioxidant activity intact. Additionally, this work also proved that the
580 obtained gelatin capsules were capable of stabilizing EGCG against degradation in
581 aqueous solution (pH = 7.4), as its antioxidant activity was better preserved in this
582 media when encapsulated than in its free form. This stabilization can be attributed to
583 both the delay of its dissolution in aqueous media, as observed in the *in-vitro* EGCG
584 release assays, and to the intermolecular interactions which were established between
585 the active molecule and its encapsulating matrix. The overall results presented in this
586 work demonstrate, for the first time, the potential of electrosprayed gelatin particles to
587 be used as encapsulation matrices for polyphenols with application in the development
588 of functional foods.
589
590 **Acknowledgements**
591 Laura G. Gómez-Mascaraque is recipient of a predoctoral contract from the Spanish
592 Ministry of Economy and Competitiveness (MINECO), Call 2013. The authors would
593 like to thank the Spanish MINECO project AGL2012-30647 for financial support.
594
595 **REFERENCES**
596 Aewsiri, T., Benjakul, S., Visessanguan, W., Wierenga, P. A., & Gruppen, H. (2010).
597 Antioxidative activity and emulsifying properties of cuttlefish skin gelatin–tannic acid
598 complex as influenced by types of interaction. *Innovative Food Science & Emerging*
599 *Technologies, 11*(4), 712-720.
600 Aquino, F. M., Melo, D. M. A., Pimentel, P. M., Braga, R. M., Melo, M. A. F., Martinelli, A. E., &
601 Costa, A. F. (2012). Characterization and thermal behavior of PrMO3 (M = Co or Ni)
602 ceramic materials obtained from gelatin. *Materials Research Bulletin, 47*(9), 2605-
603 2609.
604 Baner, A., Bieber, W., Figge, K., Franz, R., & Piringer, O. (1992). Alternative fatty food simulants
605 for migration testing of polymeric food contact materials. *Food Additives &*
606 *Contaminants, 9*(2), 137-148.

607 Barras, A., Mezzetti, A., Richard, A., Lazzaroni, S., Roux, S., Melnyk, P., Betbeder, D., &
608 Monfilliette-Dupont, N. (2009). Formulation and characterization of polyphenol-loaded
609 lipid nanocapsules. *International journal of pharmaceutics, 379*(2), 270-277.
610 Bhardwaj, N., & Kundu, S. C. (2010). Electrospinning: A fascinating fiber fabrication technique.
611 *Biotechnology Advances, 28*(3), 325-347.
612 Bock, N., Dargaville, T. R., & Woodruff, M. A. (2012). Electrospraying of polymers with
613 therapeutic molecules: State of the art. *Progress in Polymer Science, 37*(11), 1510-
614 1551.
615 Cooper, I., Goodson, A., & O'Brien, A. (1998). Specific migration testing with alternative fatty
616 food simulants. *Food Additives & Contaminants, 15*(1), 72-78.
617 Correia, D. M., Padrão, J., Rodrigues, L. R., Dourado, F., Lanceros-Méndez, S., & Sencadas, V.
618 (2013). Thermal and hydrolytic degradation of electrospun fish gelatin membranes.
619 *Polymer Testing, 32*(5), 995-1000.
620 Chakraborty, S., Liao, I. C., Adler, A., & Leong, K. W. (2009). Electrohydrodynamics: A facile
621 technique to fabricate drug delivery systems. *Advanced Drug Delivery Reviews, 61*(12),
622 1043-1054.
623 Doyle, B. B., Bendit, E. G., & Blout, E. R. (1975). Infrared spectroscopy of collagen and collagen-
624 like polypeptides. *Biopolymers, 14*(5), 937-957.
625 Dube, A., Ng, K., Nicolazzo, J. A., & Larson, I. (2010a). Effective use of reducing agents and
626 nanoparticle encapsulation in stabilizing catechins in alkaline solution. *Food Chemistry,*
627 *122*(3), 662-667.
628 Dube, A., Nicolazzo, J. A., & Larson, I. (2010b). Chitosan nanoparticles enhance the intestinal
629 absorption of the green tea catechins (+)-catechin and (−)-epigallocatechin gallate.
630 *European Journal of Pharmaceutical Sciences, 41*(2), 219-225.
631 Ebrahimgol, F., Tavanai, H., Alihosseini, F., & Khayamian, T. (2014). Electrosprayed recovered
632 wool keratin nanoparticles. *Polymers for Advanced Technologies, 25*(9), 1001-1007.
633 Erencia, M., Cano, F., Tornero, J. A., Macanás, J., & Carrillo, F. (2014). Resolving the
634 electrospinnability zones and diameter prediction for the electrospinning of the
635 gelatin/water/acetic acid system. *Langmuir, 30*(24), 7198-7205.
636 Fang, J.-Y., Hwang, T.-L., Huang, Y.-L., & Fang, C.-L. (2006). Enhancement of the transdermal
637 delivery of catechins by liposomes incorporating anionic surfactants and ethanol.
638 *International journal of pharmaceutics, 310*(1), 131-138.
639 Folch-Cano, C., Jullian, C., Speisky, H., & Olea-Azar, C. (2010). Antioxidant activity of inclusion
640 complexes of tea catechins with β-cyclodextrins by ORAC assays. *Food Research*
641 *International, 43*(8), 2039-2044.

642 Fu, N., Zhou, Z., Jones, T. B., Tan, T. T., Wu, W. D., Lin, S. X., Chen, X. D., & Chan, P. P. (2011).
643 Production of monodisperse epigallocatechin gallate (EGCG) microparticles by spray
644 drying for high antioxidant activity retention. *International journal of pharmaceutics,*
645 *413*(1-2), 155-166.
646 Gallagher, K. M., & Corrigan, O. I. (2000). Mechanistic aspects of the release of levamisole
647 hydrochloride from biodegradable polymers. *Journal of Controlled Release, 69*(2), 261-
648 272.
649 Gomes, S. R., Rodrigues, G., Martins, G. G., Henriques, C. M. R., & Silva, J. C. (2013). In vitro
650 evaluation of crosslinked electrospun fish gelatin scaffolds. *Materials Science and*
651 *Engineering: C, 33*(3), 1219-1227.
652 Gupta, P., Elkins, C., Long, T. E., & Wilkes, G. L. (2005). Electrospinning of linear homopolymers
653 of poly(methyl methacrylate): exploring relationships between fiber formation,
654 viscosity, molecular weight and concentration in a good solvent. *Polymer, 46*(13),
655 4799-4810.
656 Higuchi, T. (1961). Rate of release of medicaments from ointment bases containing drugs in
657 suspension. *Journal of Pharmaceutical Sciences, 50*(10), 874-875.
658 Hu, B., Ting, Y., Zeng, X., & Huang, Q. (2013). Bioactive Peptides/Chitosan Nanoparticles
659 Enhance Cellular Antioxidant Activity of (-)-Epigallocatechin-3-gallate. *Journal of*
660 *Agricultural and Food Chemistry, 61*(4), 875-881.
661 Huang, Z.-M., Zhang, Y. Z., Ramakrishna, S., & Lim, C. T. (2004). Electrospinning and mechanical
662 characterization of gelatin nanofibers. *Polymer, 45*(15), 5361-5368.
663 Inamura, P. Y., Kraide, F. H., Drumond, W. S., de Lima, N. B., Moura, E. A. B., & del Mastro, N. L.
664 (2013). Ionizing radiation influence on the morphological and thermal characteristics
665 of a biocomposite prepared with gelatin and Brazil nut wastes as fiber source.
666 *Radiation Physics and Chemistry, 84*(0), 66-69.
667 Jaworek, A., & Sobczyk, A. T. (2008). Electrospraying route to nanotechnology: An overview.
668 *Journal of Electrostatics, 66*(3–4), 197-219.
669 Ki, C. S., Baek, D. H., Gang, K. D., Lee, K. H., Um, I. C., & Park, Y. H. (2005). Characterization of
670 gelatin nanofiber prepared from gelatin–formic acid solution. *Polymer, 46*(14), 5094-
671 5102.
672 Klossner, R. R., Queen, H. A., Coughlin, A. J., & Krause, W. E. (2008). Correlation of Chitosan's
673 Rheological Properties and Its Ability to Electrospin. *Biomacromolecules, 9*(10), 2947-
674 2953.

675 Lai, J.-Y. (2013). Influence of solvent composition on the performance of carbodiimide cross-
676 linked gelatin carriers for retinal sheet delivery. *Journal of Materials Science: Materials*
677 *in Medicine, 24*(9), 2201-2210.
678 Larsen, C. A., & Dashwood, R. H. (2009). Suppression of Met activation in human colon cancer
679 cells treated with (−)-epigallocatechin-3-gallate: Minor role of hydrogen peroxide.
680 *Biochemical and Biophysical Research Communications, 389*(3), 527-530.
681 Larsen, C. A., & Dashwood, R. H. (2010). (−)-Epigallocatechin-3-gallate inhibits Met signaling,
682 proliferation, and invasiveness in human colon cancer cells. *Archives of Biochemistry*
683 *and Biophysics, 501*(1), 52-57.
684 Li, J.-H., Miao, J., Wu, J.-L., Chen, S.-F., & Zhang, Q.-Q. (2014). Preparation and characterization
685 of active gelatin-based films incorporated with natural antioxidants. *Food*
686 *Hydrocolloids, 37*(0), 166-173.
687 Li, Y., Lim, L. T., & Kakuda, Y. (2009). Electrospun zein fibers as carriers to stabilize (-)-
688 epigallocatechin gallate. *Journal of food science, 74*(3), C233-C240.
689 López-Rubio, A., & Lagaron, J. M. (2011). Improved incorporation and stabilisation of β-
690 carotene in hydrocolloids using glycerol. *Food Chemistry, 125*(3), 997-1004.
691 López-Rubio, A., & Lagaron, J. M. (2012). Whey protein capsules obtained through
692 electrospraying for the encapsulation of bioactives. *Innovative Food Science &*
693 *Emerging Technologies, 13*(0), 200-206.
694 López-Rubio, A., Sanchez, E., Wilkanowicz, S., Sanz, Y., & Lagaron, J. M. (2012). Electrospinning
695 as a useful technique for the encapsulation of living bifidobacteria in food
696 hydrocolloids. *Food Hydrocolloids, 28*(1), 159-167.
697 Nagarajan, M., Benjakul, S., Prodpran, T., Songtipya, P., & Nuthong, P. (2013). Film forming
698 ability of gelatins from splendid squid (Loligo formosana) skin bleached with hydrogen
699 peroxide. *Food Chemistry, 138*(2–3), 1101-1108.
700 Nagiah, N., Madhavi, L., Anitha, R., Srinivasan, N., & Sivagnanam, U. (2013). Electrospinning of
701 poly (3-hydroxybutyric acid) and gelatin blended thin films: fabrication,
702 characterization, and application in skin regeneration. *Polymer Bulletin, 70*(8), 2337-
703 2358.
704 Nieuwland, M., Geerdink, P., Brier, P., van den Eijnden, P., Henket, J. T. M. M., Langelaan, M. L.
705 P., Stroeks, N., van Deventer, H. C., & Martin, A. H. (2013). Food-grade electrospinning
706 of proteins. *Innovative Food Science & Emerging Technologies, 20*(0), 269-275.
707 Okutan, N., Terzi, P., & Altay, F. (2014). Affecting parameters on electrospinning process and
708 characterization of electrospun gelatin nanofibers. *Food Hydrocolloids, 39*, 19-26.

709 Peña, C., de la Caba, K., Eceiza, A., Ruseckaite, R., & Mondragon, I. (2010). Enhancing water
710 repellence and mechanical properties of gelatin films by tannin addition. *Bioresource*
711 *Technology, 101*(17), 6836-6842.
712 Peppas, N. A., & Sahlin, J. J. (1989). A simple equation for the description of solute release. III.
713 Coupling of diffusion and relaxation. *International journal of pharmaceutics, 57*(2),
714 169-172.
715 Pérez-Masiá, R., Lagaron, J., & López-Rubio, A. (2014). Development and Optimization of Novel
716 Encapsulation Structures of Interest in Functional Foods Through Electrospraying. *Food*
717 *and Bioprocess Technology, 7*(11), 3236-3245.
718 Re, R., Pellegrini, N., Proteggente, A., Pannala, A., Yang, M., & Rice-Evans, C. (1999).
719 Antioxidant activity applying an improved ABTS radical cation decolorization assay.
720 *Free Radical Biology and Medicine, 26*(9–10), 1231-1237.
721 Ritger, P. L., & Peppas, N. A. (1987). A simple equation for description of solute release I.
722 Fickian and non-fickian release from non-swellable devices in the form of slabs,
723 spheres, cylinders or discs. *Journal of Controlled Release, 5*(1), 23-36.
724 Robb, C., Geldart, S., Seelenbinder, J., & Brown, P. (2002). ANALYSIS OF GREEN TEA
725 CONSTITUENTS BY HPLC-FTIR. *Journal of liquid chromatography & related*
726 *technologies, 25*(5), 787-801.
727 Rocha, S., Generalov, R., do Carmo Pereira, M., Peres, I., Juzenas, P., & Coelho, M. A. (2011).
728 Epigallocatechin gallate-loaded polysaccharide nanoparticles for prostate cancer
729 chemoprevention. *Nanomedicine, 6*(1), 79-87.
730 Roussenova, M., Enrione, J., Diaz-Calderon, P., Taylor, A. J., Ubbink, J., & Alam, M. A. (2012). A
731 nanostructural investigation of glassy gelatin oligomers: molecular organization and
732 interactions with low molecular weight diluents. *New Journal of Physics, 14*(3), 035016.
733 Ru, Q., Yu, H., & Huang, Q. (2010). Encapsulation of epigallocatechin-3-gallate (EGCG) using oil-
734 in-water (O/W) submicrometer emulsions stabilized by ι-carrageenan and β-
735 lactoglobulin. *Journal of Agricultural and Food Chemistry, 58*(19), 10373-10381.
736 Shenoy, S. L., Bates, W. D., Frisch, H. L., & Wnek, G. E. (2005). Role of chain entanglements on
737 fiber formation during electrospinning of polymer solutions: good solvent, non-specific
738 polymer–polymer interaction limit. *Polymer, 46*(10), 3372-3384.
739 Shpigelman, A., Cohen, Y., & Livney, Y. D. (2012). Thermally-induced β-lactoglobulin–EGCG
740 nanovehicles: Loading, stability, sensory and digestive-release study. *Food*
741 *Hydrocolloids, 29*(1), 57-67.

742 Siepmann, J., & Peppas, N. A. (2012). Modeling of drug release from delivery systems based on
743 hydroxypropyl methylcellulose (HPMC). *Advanced Drug Delivery Reviews, 64*(SUPPL.),
744 163-174.
745 Singh, A., Sharma, P. K., & Majumdar, D. K. (2013). Development and validation of new HPLC-
746 methods for estimation of fluconazole in different simulated biological fluids: a
747 comparative study. *Journal of liquid chromatography & related technologies, 37*(4),
748 594-607.
749 Singh, B. N., Shankar, S., & Srivastava, R. K. (2011). Green tea catechin, epigallocatechin-3-
750 gallate (EGCG): Mechanisms, perspectives and clinical applications. *Biochemical*
751 *Pharmacology, 82*(12), 1807-1821.
752 Singh, R., Akhtar, N., & Haqqi, T. M. (2010). Green tea polyphenol epigallocatechi3-gallate:
753 Inflammation and arthritis. *Life Sciences, 86*(25-26), 907-918.
754 Song, J.-H., Kim, H.-E., & Kim, H.-W. (2008). Production of electrospun gelatin nanofiber by
755 water-based co-solvent approach. *Journal of Materials Science: Materials in Medicine,*
756 *19*(1), 95-102.
757 Songchotikunpan, P., Tattiyakul, J., & Supaphol, P. (2008). Extraction and electrospinning of
758 gelatin from fish skin. *International Journal of Biological Macromolecules, 42*(3), 247-
759 255.
760 Spizzirri, U. G., Hampel, S., Cirillo, G., Nicoletta, F. P., Hassan, A., Vittorio, O., Picci, N., &
761 Iemma, F. (2013). Spherical gelatin/CNTs hybrid microgels as electro-responsive drug
762 delivery systems. *International journal of pharmaceutics, 448*(1), 115-122.
763 Steinmann, J., Buer, J., Pietschmann, T., & Steinmann, E. (2013). Anti-infective properties of
764 epigallocatechin-3-gallate (EGCG), a component of green tea. *British journal of*
765 *pharmacology, 168*(5), 1059-1073.
766 Strauss, G., & Gibson, S. M. (2004). Plant phenolics as cross-linkers of gelatin gels and gelatin-
767 based coacervates for use as food ingredients. *Food Hydrocolloids, 18*(1), 81-89.
768 Tola, Y. B., & Ramaswamy, H. S. (2014). Combined effects of high pressure, moderate heat and
769 pH on the inactivation kinetics of Bacillus licheniformis spores in carrot juice. *Food*
770 *Research International, 62*(0), 50-58.
771 Wulansari, R., Mitchell, J. R., Blanshard, J. M. V., & Paterson, J. L. (1998). Why are gelatin
772 solutions Newtonian? *Food Hydrocolloids, 12*(2), 245-249.
773
774

775 **Table 1.** Gelatin concentrations tested and their optimal processing parameters.

776

777

Sample Code	[Gelatin] (% w/v)	Flow rate (mL/h)	Voltage (kV)
Gel20	20	0.15	28
Gel10	10	0.5	20
Gel8	8	0.2	15
Gel5	5	0.2	17

778

779

780

781

782 **Table 2.** Onset temperature, temperatures of maximum degradation rate and
783 corresponding weight losses of the two degradation stages for unprocessed EGCG and
784 gelatin, and for the e-sprayed particles

Sample	T_{onset} (ºC)	T_{max1} [a] (ºC)	WL_1 [b] (%)	T_{max2} [a] (ºC)	WL_2 [b]
Gelatin	265.6	301.3	45.2	537.7	36.9
EGCG	228.8	235.4	33.7	483.9	62.3
Gel8	241.3	324.4	53.7	531.8	34.5
Gel8-EGCG	235.8	321.6	50.2	534.4	37.0

785 [a] Temperature of maximum degradation rate
786 [b] Weight loss of the corresponding degradation stage
787

788 **Table 3.** EGCG release kinetic parameters (k_i) and the linear correlation coefficients
789 (R^2)

790

791

792

Release medium	k_1 ($h^{-0.425}$)	k_2 ($h^{-0.850}$)	R^2
Ethanol 96%	0.10±0.01	-0.006±0.002	0.98
MES	0.42±0.02	-0.053±0.006	0.99
PBS	0.35±0.04	-0.043±0.007	0.95

793

794

795

796

797 **Figure captions**

798 **Figure 1.** Schematic chemical structures of raw materials: a) gelatin and b) EGCG

799 **Figure 2.** Electrical conductivity, surface tension and rheological behaviour of gelatin
800 solutions in diluted acetic acid (20% v/v). Properties of gelatin solution containing
801 EGCG are also shown (emphasised by arrows).

802 **Figure 3.** SEM images of gelatin structures obtained through electrohydrodynamic
803 processing of aqueous solutions with different protein concentrations (left) and particle
804 size distributions for the e-sprayed samples (right). The image and size distribution at
805 the bottom correspond to EGCG-loaded capsules. Scale bars in SEM images correspond
806 to 2 μm. Asterisk (*) depicts significant differences for the particle size distribution ($p <$
807 0.05).

808 **Figure 4.** Infrared spectra of commercial and e-sprayed materials in the region from
809 1800 to 800 cm^{-1}. Arrows indicate bands corresponding to EGCG. The whole spectra
810 are depicted in the inset, where arrows indicate band displacements.

811 **Figure 5.** DTG curves of raw EGCG and gelatin, and e-sprayed particles

812 **Figure 6.** EGCG release profiles from e-sprayed gelatin particles in a) ethanol, b) MES
813 and c) PBS

814 **Figure 7.** Degradation profiles of free and encapsulated EGCG in PBS. Asterisk (*)
815 depicts significant differences between the two samples at each time point ($p < 0.05$).

816

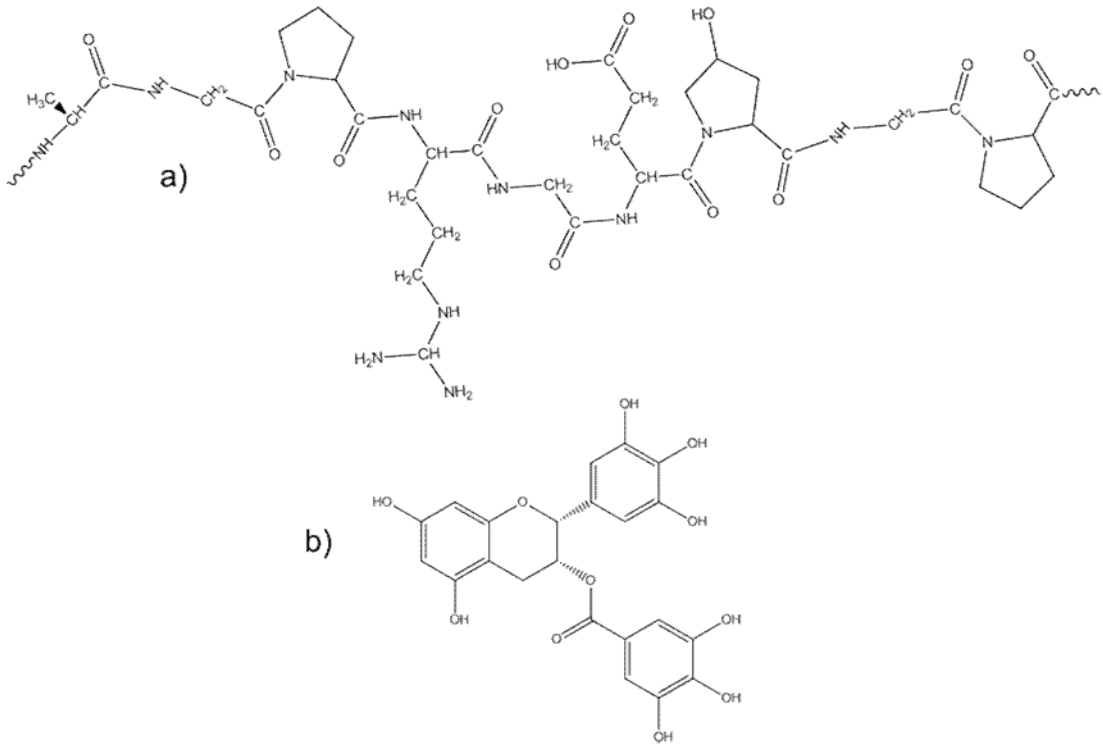

817

818 **FIGURE 1.**

819

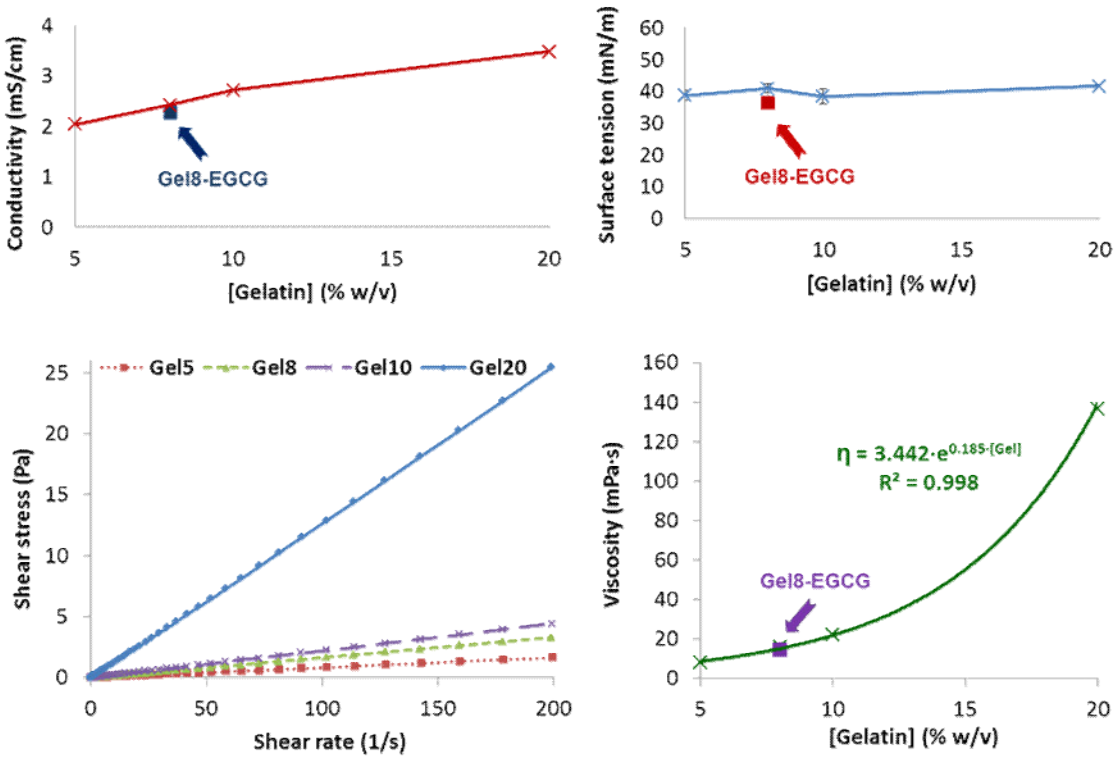

820

821 **FIGURE 2.**

822

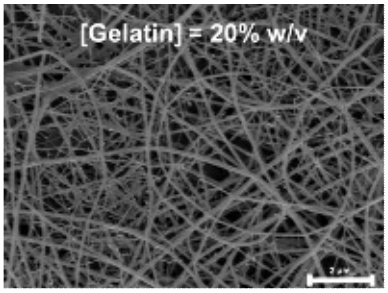

Sample	Gel5 (*)	Gel8	Gel10	Gel8-EGCG
Mean diameter (μm)	0.23	0.48	0.49	0.47
Standard deviation (μm)	0.17	0.38	0.40	0.37
Minimum diameter (μm)	0.05	0.06	0.07	0.07
Maximum diameter (μm)	0.88	1.84	2.12	2.00

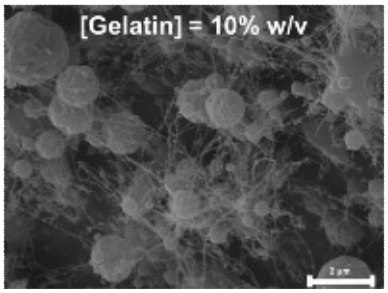

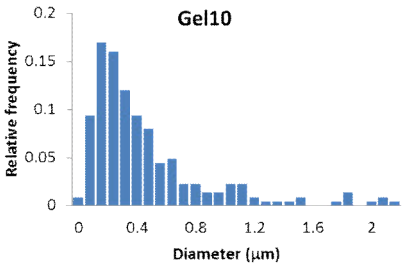

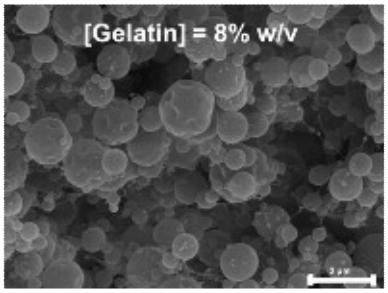

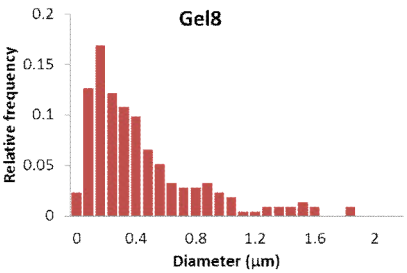

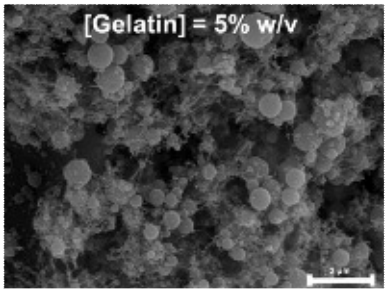

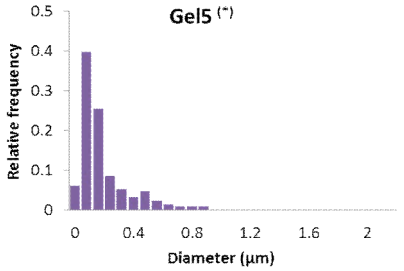

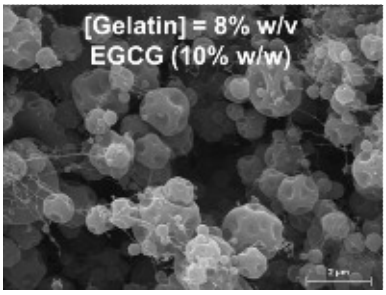

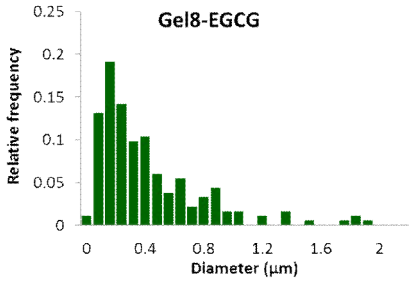

FIGURE 3.

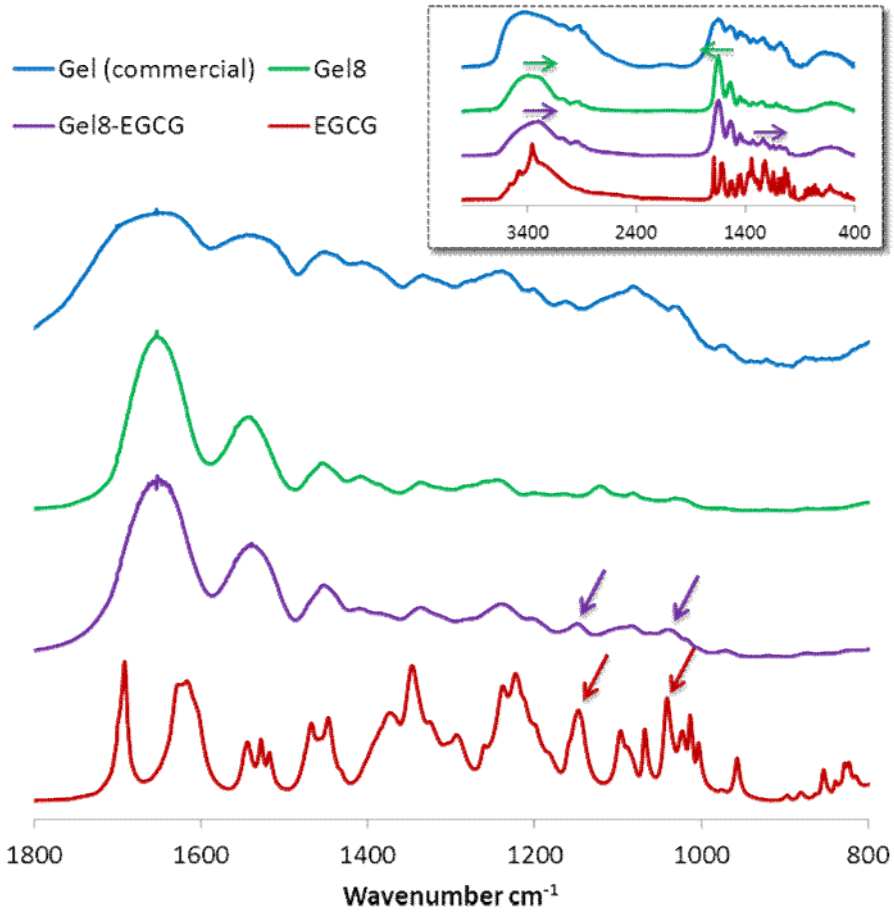

826

827 FIGURE 4.

828

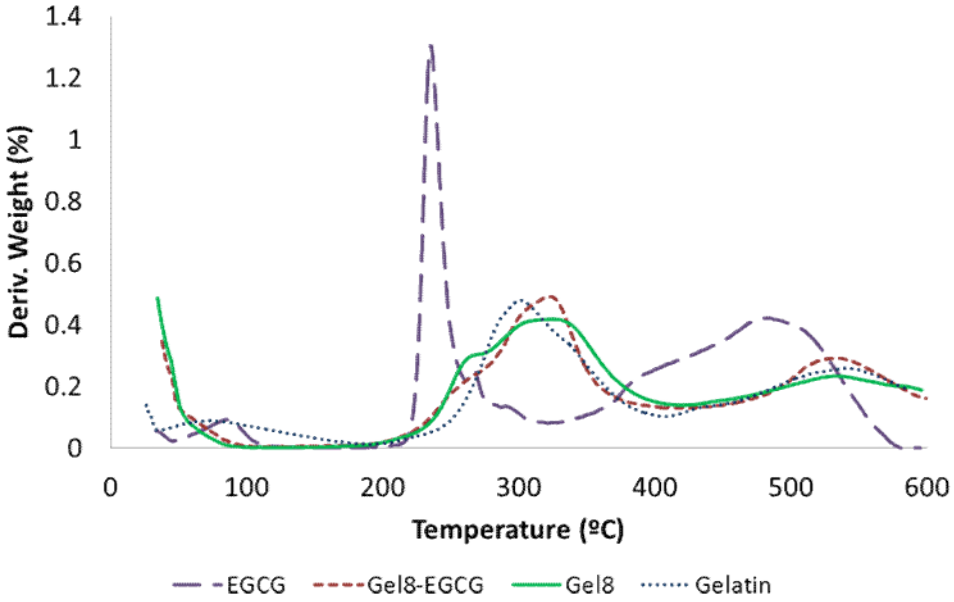

829

830 FIGURE 5.

831

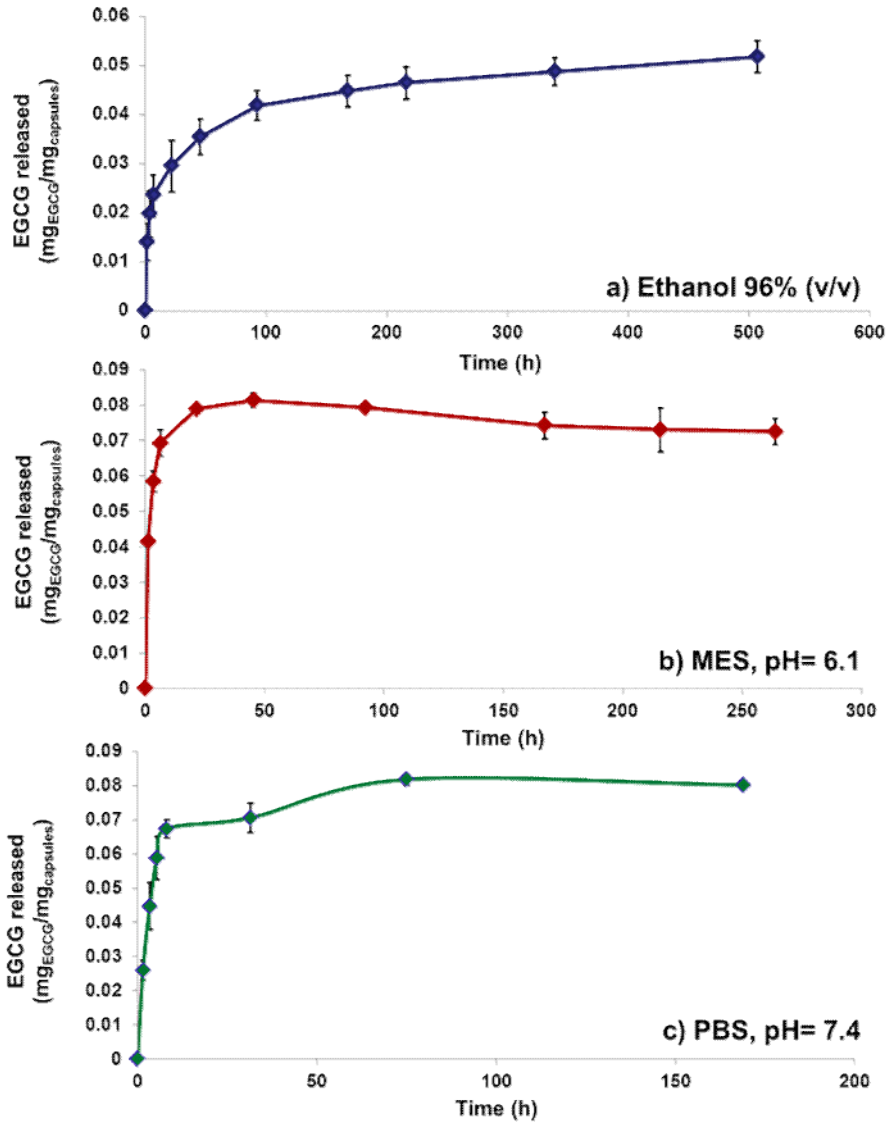

832

833 FIGURE 6.

834

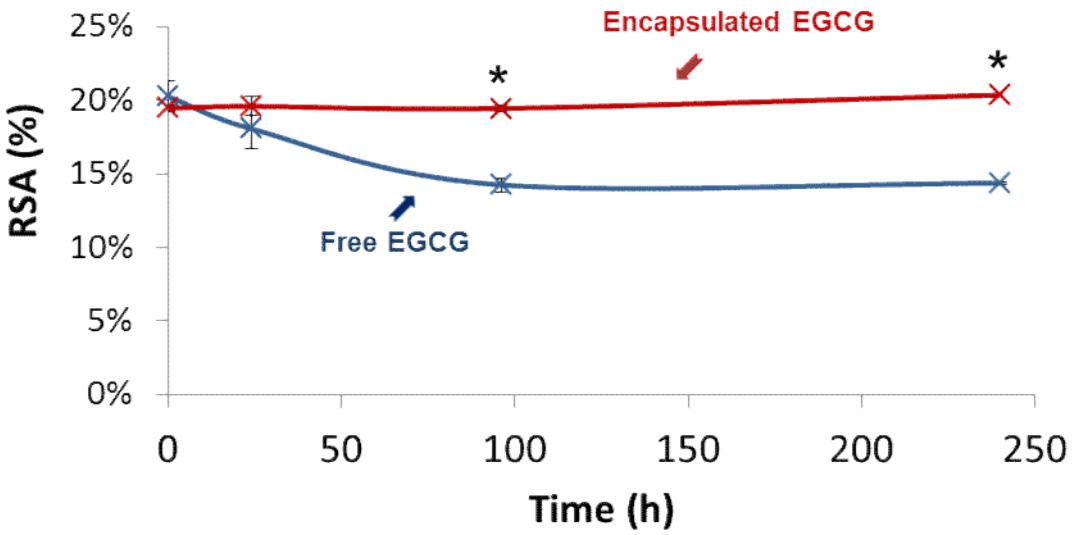

835

836 FIGURE 7.

837

Highlights

- Gelatin capsules were obtained through electropraying for bioactive protection
- (–)-Epigallocatechin gallate (EGCG) was encapsulated in the electrosprayed capsules
- Encapsulation efficiencies close to 100% were achieved
- The antioxidant activity of the bioactive was kept during electrospraying
- Electrosprayed gelatin capsules effectively protected EGCG against degradation

850 **Supplementary Material**

851

852

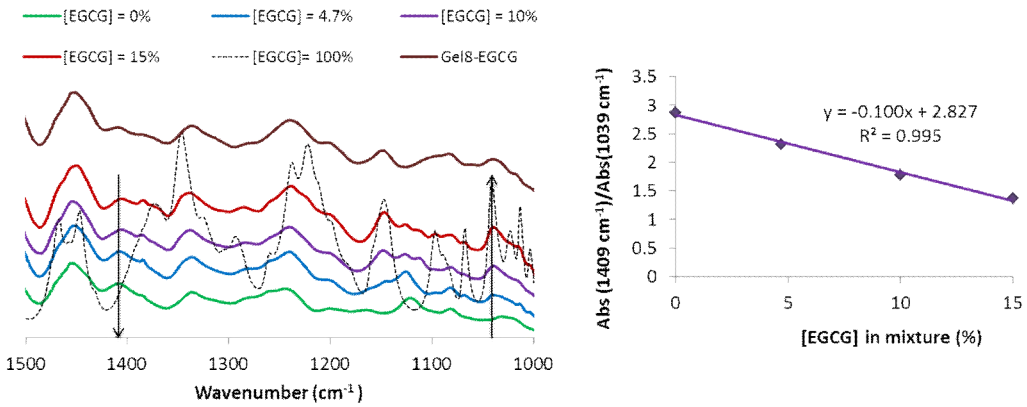

853

854

855 **Figure S1.** FTIR spectra of KBr pellets used for the calibration curve containing
856 different proportions of gelatin and EGCG (left) and the corresponding calibration curve
857 (right). The spectrum from the EGCG-containing capsules is also included. Arrows
858 point out the intensity changes of the selected bands.

859

860